scientific reports

Check for updates

OPEN

Tracking EEG network dynamics through transitions between eyes-closed, eyes-open, and task states

Paweł Krukow[1✉], Victor Rodríguez-González[2,3], Natalia Kopiś-Posiej[1], Carlos Gómez[2,3] & Jesús Poza[2,3,4]

Our study aimed to verify the possibilities of effectively applying chronnectomics methods to reconstruct the dynamic processes of network transition between three types of brain states, namely, eyes-closed rest, eyes-open rest, and a task state. The study involved dense EEG recordings and reconstruction of the source-level time-courses of the signals. Functional connectivity was measured using the phase lag index, and dynamic analyses concerned coupling strength and variability in alpha and beta frequencies. The results showed significant and dynamically specific transitions regarding processes of eyes opening and closing and during the eyes-closed-to-task transition in the alpha band. These observations considered a global dimension, default mode network, and central executive network. The decrease of connectivity strength and variability that accompanied eye-opening was a faster process than the synchronization increase during eye-opening, suggesting that these two transitions exhibit different reorganization times. While referring the obtained results to network studies, it was indicated that the scope of potential similarities and differences between rest and task-related networks depends on whether the resting state was recorded in eyes closed or open condition.

Keywords Neural networks, Chronnectomics, EEG, Functional connectivity, Default mode network

The finding that baseline neuronal settings exhibit the characteristics of an organization enabling the valid prediction regarding cognitive performance reinforces the question of the differences and similarities between network configurations at rest and during different tasks[1–4]. Although it seems intuitively obvious that the functioning of the resting brain differs from the activity associated with in exogenous information processing, network research outcomes are still ambiguous in this matter. Comparisons of rest and task-dependent brain behavior suggest differences in the neural network, revealed with graph theory-related metrics, such as global efficiency, clustering coefficient, and modularity[2,5], but also in terms of the number of highly-connected hubs[1] and the overall level of functional connectivity strength[6]. According to Arbabshirani and co-workers[7] suggestion, task-related brain states, compared with resting-state networks, are associated with lower synchronization strength, but the spread of connected regions rises, probably enabling the wider recruitment of areas specialized in a given task processing. On the other hand, a vast scope of network studies concludes that rest and task brain activity patterns are very similar[8,9].

One of the important issues in the neuroscientific research on spontaneous and task-related neural activity is the heterogeneity of methodological solutions concerning the resting condition. This bears on *inter alia*, to the problem of recording the resting-state in eyes closed or eyes open conditions and treating both of these settings as equivalent[10]. A series of researches showed unequivocally that the neuronal configurations in these two conditions are different (see a short summary in Weng et al.[11]). Agcaoglu and co-workers[12], in a large group of children, showed that in the eyes open condition with eyes fixed in an object (EO-F), neuronal areas belonging to the visual network were strongly synchronized. On the other hand, connectivity between auditory and sensorimotor network was higher in the eyes closed (EC) state[12]. It has been also reported that coupling between the default

[1]Department of Clinical Neuropsychiatry, Medical University of Lublin, Ul. Głuska 1, 20-439 Lublin, Poland. [2]Biomedical Engineering Group, University of Valladolid, Valladolid, Spain. [3]Centro de Investigación Biomédica en Red de Bioingeniería, Biomateriales y Nanomedicina (CIBER-BBN), Instituto de Salud Carlos III, Madrid, Spain. [4]IMUVA, Instituto de Investigación en Matemáticas, University of Valladolid, Valladolid, Spain. ✉email: pawelkrukow@umlub.pl

mode network (DMN) and sensorimotor network is higher in EC than in EO[10]. These authors assumed that the correlation between the functioning of the primary visual cortex (V1 area) and the rest of the brain should significantly differentiate network patterns in EC and EO states; they also found that EC is associated with significantly greater communication between V1 and the DMN, while EO induces a stronger relationship between the V1 cortex and the salience network (SN). Similar results were obtained by other researchers[13]: stronger connectivity between V1 and SN in EO condition suggests that this state represents a relatively substantial level of the brain's readiness to cope with incoming external stimuli. Other studies showed that EC and EO also differ in terms of the dynamic arrangement of the neural network[14]. Using analytical solutions to capture the range of variation in functional connectivity (FC) strength and topography, the results were somewhat similar to those mentioned earlier, indicating stronger coupling between the sensorimotor and auditory networks in the EC state. EC and EO have also been shown to generate different compositions of repetitive connection patterns (microstates) spanning multiple major functional networks[15]. Without referring in detail to specific functional networks, Wang et al.[16] documented that EC, compared to EO, is a mode with a higher number of transitions between various patterns of connectivity, and represents a brain tendency to remain longer in a hyper-connected condition. Summing up, it can be concluded that the differences in the EC and EO brain states seem to be even more notable than in the case of comparisons between the broadly understood resting-state and task-related activity. This means that the transition between these conditions, as well as the transition between the resting-state (especially in the EC condition) and starting the task, should be associated with significant changes at many levels of neuronal activity, including the strength of synchronization itself.

Many computational tools have been developed to grasp a time-varying arrangements of inter-neuronal synchronizations[17,18]. Chronnectomic research (i.e., the study of time-varying brain networks) has corroborated that the dynamic aspects of network orchestrations designate specific processes and clinical conditions[19–21]. These studies reported that brain activity is a set of transient, though reoccurring, connectivity states and meta-states, which can be identified and analyzed. The vast majority of connectomic and chronnectomic studies conducted so far were aimed at recognizing dynamic patterns typical for a given condition (e.g., resting-state) or differentiating specific groups (e.g., healthy controls *versus* patients), but not at analyzing neural transitions between these states. Although there are accessible studies on network "reorganization", "modulation", or "reconfiguration"[22,23], they consisted of comparisons of two or more stationary patterns of neuronal activity arrangements and only indirectly inferred how such a transition occurs. It seems plausible that such an approach stems from the fact these and similar studies were conducted using functional magnetic resonance imaging (fMRI), a technique with a relatively low temporal resolution that prevents the observation of probably fast neuronal activity during transition processes. However, neurophysiological methods, such as electroencephalography (EEG) and magnetoencephalography (MEG), have the ability to capture the oscillatory activity of neurons on a much more precise time scale[24].

Considering the above, the aim of the current study was to verify whether it is possible to track the continual dynamics of between-state connectivity transitions with reference to two processes: transition between closed and open eyes and transition between resting-state and task-state. Although we refer to the analyses described earlier, our study differs fundamentally from the previous ones in that we want to preserve the continuity of connectivity modulations ongoing during transitions. So far, even in studies assessing the connectivity with reference to its temporal changes, the focus was rather on the connectivity stability or the span length of remaining in a given synchronization state (the so-called *'dwelling time'*)[25], while the problem of how a given process is organized in the time dimension regarding the sequence of successive processes was somewhat omitted. We want to establish whether it is possible to identify any distinct phases appearing in between-states transition, how fast one activity pattern (e.g., typical for resting-state) turns into the opposite (e.g., typical for task-state), and if there are clear patterns of changes in the strength of functional connections that may differ between analyzed transitions. In addition to the expected fluctuations in connectivity strength during transitions, we also intend to reconstruct the potential dynamics of strength variability. Whether the scope of coupling's intra- and inter-individual variability expresses any dynamics due to modifying factors or is a non-changeable trait is still an open question[12,26]; we assume that its potential dynamics might add another insight into the temporal organization of between-states transition. Expected changes in the connectivity strength and its variability were assessed at the global level, but also with reference to selected functional networks having, at least to some extent, opposite characteristics regarding their activation modes during rest or task conditions[27]. In our analysis, we took into account selected frequencies (i.e., alpha and beta), omitting the lowest ones (i.e., delta and theta), in order to obtain data with an appropriate level of temporal granulation, necessary to reproduce the transition process. A task state has been elicited by the performance of a n-back test with a relatively low level of difficulty. Such type of task was chosen to engage participants in activities requiring continuous attention to external stimuli, visual differentiation regarding test material, and fast psychomotor responses, but at the same, not to expose them to a difficult task, the performance of which could trigger uncontrolled affective reactions, e.g. related to failure anxiety or frustration caused by frequent errors. As Klein and co-workers documented[28], exposure to cognitive tasks perceived by participants as complicated, evokes the activity of neural networks related to affective arousal and alterations in the functioning of the autonomic system[29]. Inducing such reactions would introduce neural activity being a confounding factor in the neural network analysis.

Materials and methods
Participants
The study involved recruitment of a right-handed volunteers (males and females) in possession of normal or corrected-to-normal vision, aged between 21 and 25 years. All participants gave their written consent to participate in the study. Subjects declared that they did not take medications prescribed by a psychiatrist or neurologist.

Before EEG procedure participants were tested for fluid intelligence using the Raven's Standard Progressive Matrices (RSPM) test[30] in polish psychometric adaptation[31]. The study was approved by the Research Team's University Ethics Committee and was conducted in accordance with the Declaration of Helsinki.

Procedure

Participants sat in a comfortable chair in a dimly light room. The entire study consisted of 2 major blocks. Each block consisted of 10 'cycles' containing a cognitive task (1-Back) and two types of resting-state (EO and EC). The first block started with EC-rest, followed by EO-rest and then a task, the second block started with a task, followed by EO rest which was followed by EC rest. Such an arrangement of experimental procedure enabled recording transitions between all involved rest and task states (Fig. 1). During the whole study, the blocks appeared in random order. Also, because one of the resting-state conditions used in the study was EC, participants heard a sound announcing every time the "state" changed (e.g., from EC to EO, from EC to 1-Back). Additionally, before every 1-Back procedure, for 2 s, participants saw the "Get ready" information displayed on the screen. The whole study took about 35 min for every participant.

Before starting the experiment, participants were informed about the 1-Back task and the resting-state recordings. After that, participants had to perform a training with the 1-Back procedure and resting-state. Only during the training participants saw the feedback ("Correct" or "Incorrect") announcing if their response to the target or non-target letter was right. In 1-Back tasks, participants viewed letters successively presented on a screen. They had to react to every letter to indicate whether the letter was a target or a non-target. The target was the same letter as the one before. When participants saw the target, they had to press the red button (right "ctrl" on the keyboard) and for the non-target, they had to press the blue button (left "ctrl"). The 1-Back task took about 1 min. The letters used in the procedure were black (font style: Ariel, approximately 3 cm high). Letters were presented on a gray background (RGB 128, 128,128), singly for 200 ms until participant response. All participants were presented with the same number of letters in a given 1-Back trial. In all conditions, 40% of letters were targets. The one 1-Back block took about one minute.

In the resting-state tasks, participants had to close or open their eyes depending on the information viewed on the screen. During the resting-state, participants were instructed to sit still until they heard the sound ending the task. They were also instructed that the resting-state blocks are not breaks, so they must keep movement to a minimum. However, participants did not get specific instructions on what they should think about during the resting-state. The participants had to sit for 40 s with their eyes closed and 40 s with their eyes open.

EEG acquisition and preprocessing

For the signal acquisition, 64 active electrodes (ActiCAP, Brain Products, Munich, Germany) connected to a high-input-impedance amplifier (200 MΩ, GES 300, Electrical Geodesics, Inc., Eugene, OR) were used. The EEG was referenced to FCz electrode and digitized at a sampling rate of 500 Hz. Electrode impedances were kept below 5 kΩ.

Offline signal processing included: (i) re-reference to common average reference; (ii) band-pass finite impulse response (FIR) filtering in the range 0.1–45 Hz; (iii) interpolation of bad channels by means of the artifact sub-space reconstruction method; iv) muscle and ocular artifact rejection using independent component analysis (ICA); (v) segmentation into epochs of 11 s, which begin 3 s before the transition between states and extend 8 s after it (i.e., $[-3\ 8]$ seconds). Crucially, all the subsequent analyses were conducted filtering the signals in the alpha (8–13 Hz) and beta bands (13–30 Hz), due to the premises mentioned earlier.

Source inversion

In order to reduce the volume conduction effects and obtain more accurate estimations about the neural networks, the source level time-courses of the signals were reconstructed[32,33]. To this end, we used the standardized low-resolution brain electromagnetic tomography (sLORETA) algorithm[34]. The sLORETA algorithm is designed to constrain solutions by assuming that nearby neurons are synchronized, resulting in maximal correlation between neighboring sources. This approach helps to estimate the most likely locations of neural sources responsible for the recorded EEG signals. Besides, this algorithm has been broadly applied in EEG studies, so its performance with this type of signals has been already demonstrated[35–37]. For more detailed information about sLORETA and its underlying principles, you can refer to[34]. The implementation of the sLORETA algorithm is freely available in the Brainstorm toolbox (http://neuroimage.usc.edu/brainstorm)[38].
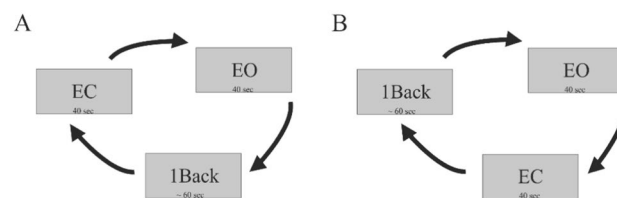

Figure 1. Illustration of the experimental procedure with two blocks. Each arrow indicates analyzed transitions between a given state.
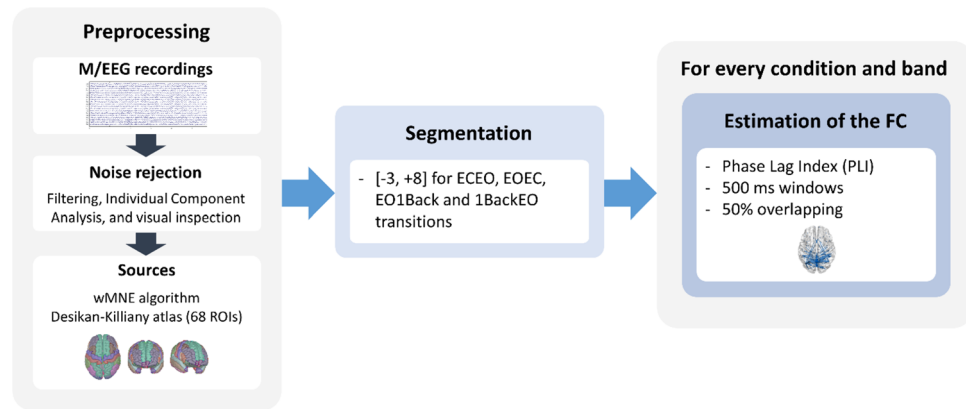
Figure 2. Flow diagram of the employed methodology to assess the functional connectivity in the assessed transitions. Preprocessing—The artifacts are removed from the EEG signals, and their source-level time courses are reconstructed. Segmentation—The signals are segmented between − 3 and + 8 s, with the 0 s being the moment when the transition between conditions is indicated. Estimation of the FC—For every trial (extracted in the previous step), and band (alpha and beta) the FC is estimated by means of PLI metric employing a 500 ms sliding window with an overlapping of 50%.

To create the forward model, the ICBM152 anatomical template was employed[39,40]. A three-layer (brain, skull, and scalp) head model was created by means of the boundary element method available in OpenMEEG software[32,41]. The source space was limited to the cortex and included 15,000 sources, which were constrained to be normal to the cortex[32]. To avoid neighboring generators to blur the results, sources in opposite directions were flipped[42]. Finally, the 15,000 sources were grouped into 68 regions of interest (ROIs), according to the Desikan-Killiany atlas[32,33,43]

EEG analyses: estimating the neural networks

There are very different ways of analyzing the FC patterns: considering the phase, with metrics as the Phase Lag Index (PLI); studying the amplitude-based couplings, with metrics as the Amplitude Envelope Correlation; or assessing the spectral distribution, with metrics as the Coherence[44]. In this study, we computed the PLI, as it has been widely used in other studies employing EEG signals, and it showed a high robustness against volume conduction effects[45–48].

Of note, we focused on evaluating the mechanisms underlying the transitions between states, such as EO, EC, and a working memory task. This analysis is intended to go beyond the evaluation of the static FC (FC) in the whole trial at a time, employing a sliding window of 500 ms with an overlap of 50%. By doing this, we assessed the dynamic FC (dFC), that is, how the brain reconfigures its resources during the transition between states.

The *Phase Lag Index* (PLI) is a connectivity metric that evaluates the consistency (in time) of the phase difference between two time series. The PLI is defined as follows[45]:

$$PLI_{i,j} = \left| \left\langle sign \left[\Delta \phi_{i,j}(t) \right] \right\rangle \right|,$$

where $|\cdot|$ represents the absolute value, $\langle \cdot \rangle$ is the mean, $sign[\cdot]$ is the signum function, and $\Delta\phi_{i,j}(t)$ is the phase difference between two time series, $x_i(t)$ and $x_j(t)$ from ROIs i and j[45]. The PLI ranges between 0 and 1, with values near "0" meaning unrelated signals, and values around "1" standing for closely coupled time series[45]. If the two signals under assessment are not coupled, the phase difference will not be consistent and, thus, the PLI value will be low. On the other hand, if the differences are consistent (the first signal is consistently ahead of the other, or

	M/%	SD/range
Age	23.25	2.15
sex	59% females	
Years of education	14.54	2.48
RSPM[a] scores:		
Raw scores	49.40	5.72
Percentiles	60.50	55–66
Wechsler-type IQ	104.50	102–106

Table 1. Demographic and cognitive characteristics of the studied sample. [a]RSPM—Raven's Standard Progressive Matrices test.
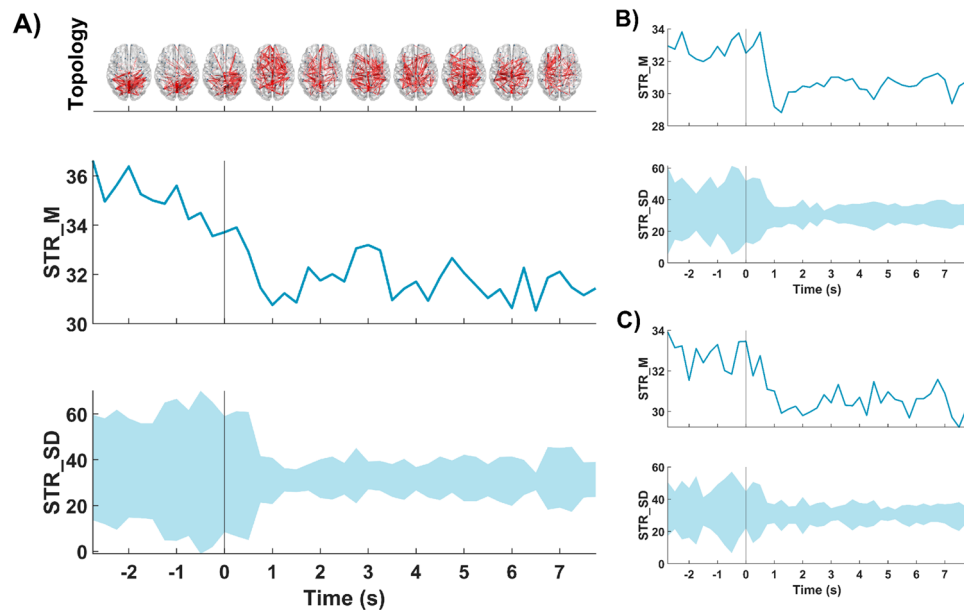
Figure 3. Evolution across time of the STR_M and STR_SD for: (**A**) global neural network, (**B**) DMN and (**C**) CEN. Within each section, in the upper row it is depicted the evolution of the STR_M, and in the lower row the evolution of the STR_SD during the ECEO transition in the alpha band. The transition between both states is marked with a vertical line (i.e., 0 s). Moreover, for the global neural network, the evolution of the topology during the transition is depicted in the upper part of the section (**A**).

vice versa), the PLI value will be high[45]. Crucially, the PLI disregards the zero-lag couplings as it considers that they are undesirable and elicited by volume conduction effects or active references[45].

In our study, dFC was computed using the sliding-window approach, considering trials of 11 s. Each trial was subdivided in overlapping windows of 500 ms (50% overlap, i.e., 250 ms). A 500 ms time window was selected to include at least 4 oscillations of the slowest frequency (8 Hz), in order to reach balance between a robust data treatment and a dynamic analysis of the functional connectivity. Finally, PLI was estimated from source level time-courses from 68 ROIs for each 500 ms window. By computing the PLI between each pair of sensors at each window of 500 ms, we defined the so-called "adjacency matrices". They are N-dimensional square matrices (with N being the number of sources or channels) that describe the statistical coupling between sensors in a specific time interval. There are lots of network-based metrics that can be extracted from these matrices in order to summarize the information they provide. In this manuscript, we have considered the connectivity strength (STR), which is defined as the average PLI value for one sensor (or source) with the other sensors (or sources):

$$STR_i = \sum_{i \neq j, j=1}^{N} PLI_{i,j}$$

STR values at each time window of 500 ms were concatenated to build time vectors that summarized the dynamics of network transitions across the trials of 11 s. Finally, changes in time-varying STR were quantified by computing the mean (central tendency) and the standard deviation (variability) for each window across trials.

Additionally, we repeated all the analyses considering only the ROIs belonging to the Default Mode Network (DMN) and to the Central Executive Network (CEN). In Table S1 of the Supplementary Material, the ROIs assigned to DMN and CEN are shown.

In Fig. 2 presents a graphical summary of this methodology, from the preprocessing step, to the final estimation of the FC.

Statistical analyses

An initial round of exploratory data analysis was conducted to assess the distribution of the data. Normality and homoscedasticity were assessed using the Lilliefors and Bartlett tests, respectively. As the data did not satisfy the assumptions of normality and homoscedasticity, non-parametric statistical tests were employed. Reaction times and the range of correct responses in the 1Back task were analyzed using analysis of variance (ANOVA). The study compares the data distribution of the participants during the transition between brain states (EC, EO, and 1-Back). As the samples for the different transitions are composed by the same subjects (thus being paired data), the Wilcoxon signed-rank test was used. The multiple comparisons problem was addressed by means of the Benjamini and Hochberg False Discovery Rate (FDR) method[49].
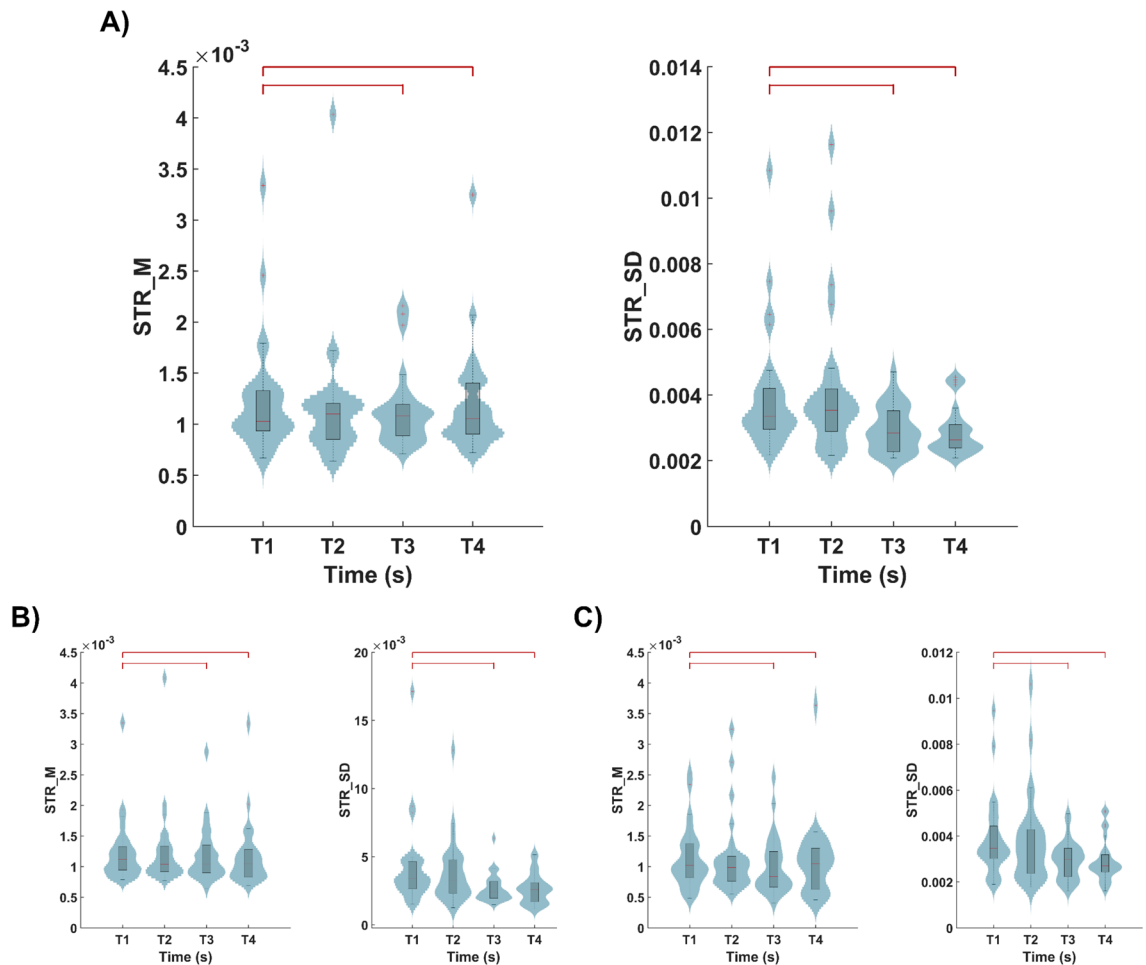
Figure 4. (**A**) Data distribution of the global network STR_M, and STR_SD during the ECEO transition in the alpha band. Analogous comparisons for the results regarding DMN and CEN are depicted in sections (**B,C**), respectively. Within each panel, the boxplots group the FC values of a different time range: from −3 to −1.5 s (T1), from −1.5 to 0 s (T2), from 0 to 1.5 s (T3), and from 3 to 4.5 s (T4). The statistically significant differences (p-value < 0.05, corrected Wilcoxon signed-rank test) are indicated with dark red lines.

Results

Participants characteristics and behavioral outcomes

During the recruitment process, a group of 35 individuals meeting the initial research criteria was gathered. After the initial analysis of the EEG recordings, the results of 5 of them were rejected due to numerous artifacts reducing the quality of the outcomes. Additionally, data from two subjects were discarded due to a high number of errors during task performance. Outcomes from another person were also removed due to RPM test scores much above the group majority. The final group comprised 27 participants, 16 females and 11 males. Table 1 presents the group's demographic characteristics and fluid intelligence scores.

The mean accuracy during the 1-Back task was 80%. Mean reaction times from 1-Back performed after EO and EC conditions were similar: $F(1, 19) = 0.010$, $p = 0.921$, $\eta_p^2 < 0.001$. The correctness of the 1-Back task performed after the EC was significantly lower (M = 0.61, SD = 0.14 vs. M = 0.98, SD = 0.02) compared with task performed after EO: $F(1, 19) = 128.74$, $p < 0.0001$, $\eta_p^2 = 0.87$.

Functional connectivity changes during state-dependent transitions

In this study, the electrophysiological activity of the subjects has been recorded in three different conditions: EC, EO, and 1-Back. Considering these states, we posed four different scenarios: (i) transition from EC to EO (ECEO); (ii) transition from EO to EC (EOEC); (iii) transition from EO to 1-Back (EO1Back); and (iv) transition from 1-Back to EO (1BackEO). We have not extracted the EC to 1-Back transition because it contains another transition (ECEO) within. The analysis of the expected connectivity changes concerned the following dimensions: global connection strength (STR_M), global connection strength variance (STR_SD), and the same measures calculated separately for two functional networks, i.e. DMN and CEN. Of note, in the main body of the manuscript all the results showed were calculated for the activity of the alpha band (8–13 Hz). Analogous results, calculated for the beta activity (13–30 Hz) are depicted in Supplementary Material.
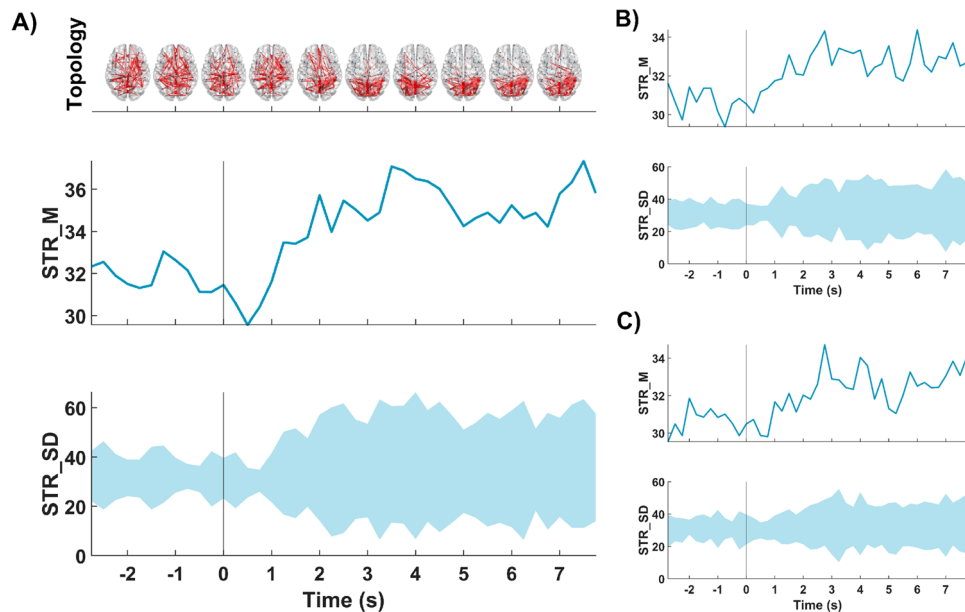
Figure 5. Evolution across time of the STR_M and STR_SD for: (**A**) global neural network, (**B**) DMN and (**C**) CEN. Within each section, in the upper row it is depicted the evolution of the STR_M, and in the lower row the evolution of the STR_SD during the EOEC transition in the alpha band. The transition between both states is marked with a vertical line (i.e., 0 s). Moreover, for the global neural network, the evolution of the topology during the transition is depicted in the upper part of the section (**A**).

ECEO transition

Figure 3 presents the temporal evolution of mean SRT_M and STR_SD for the global neural network, and also the evolution of the same measures calculated for DMN and CEN. Network topology before the transition starts (i.e., interval [− 3, 0] s) shows an occipital configuration, and just after the transition (0 s), it turns into a more homogeneous and widespread organization. During ECEO transition, STR_M and STR_SD decreased. Qualitatively, it can be appreciated that the STR transition is relatively fast, taking less than 1 s (approximately 750 ms) until the brain reaches a stable state (in terms of mean STR_M). STR_SD change seems to be slower since its drop starts from about 750 ms after the transition. Very similar processes regarding FC_{STR} and STR_SD can be observed for DMN and CEN. These transitions were also characterized by a decrease of STR_M and STR_SD.

Figure 4 illustrates the global network quantitative data distribution of mean STR_M, and STR_SD (left panel), and the same metrics regarding DMN and CEN (right panel), for four different time intervals: T1 = [− 3, − 1.5] s, T2 = [− 1.5, 0] s, T3 = [0, 1.5] s, and T4 = [3, 4.5] s. Four comparisons of the FC data distribution (in terms of STR_M and STR_SD) of different time intervals were carried out: (i) T1 with T2, to verify that the neural activity was stable (and the connectivity estimation robust, as no changes were expected); (ii) T1 with T3, to check whether changes in FC values have occurred; (iii) T1 with T4, to see whether the new configuration of the neural network has been maintained, or has returned to the original configuration (that in T1); and (iv) T3 with T4, to assess whether a new neural reconfiguration has occurred since T3. As can be appreciated in Fig. 4, statistically significant differences (p-values < 0.05, Wilcoxon signed rank test, FDR-corrected) were found between T1 and T3, and between T1 and T4, for both STR_M and STR_SD. These results confirmed a significant decrease of STR_M and STR_SD after the transition (i.e., time point 0 s) compared with the T1 interval. The same results were observed regarding time intervals comparison for DMN and CEN functional networks. In the Supplementary material, the same analyses for the beta frequency band are depicted. No qualitative and quantitative STR_M and STR_SD changes were observed.

EOEC transition

As shown in Fig. 5, the modifications in the topology of the FC patterns for the EOEC consists of gradual changes starting from a wide distribution that progressively go after the transition (time 0 s) toward an occipital-centered organization. Compared with the ECEO, the occipitally-oriented topology appears not just after the transition, but rather after the third second of transition. Mean STR_M and STR_SD increase, but the stability of STR_M starts from 2 s after the transition. A clear increase in STR_SD develops from 1 s after closing the eyes. Such an arrangement of STR_M and STR_SD dynamics concerned also DMN and CEN functional networks.

Statistical analysis of the EOEC transition revealed significant differences in global STR_M and STR_SD between intervals T3 and T4, followed by differences between T4 and T1 (Fig. 6). This means that after the transition both FC measures increased significantly. The dynamics of the CEN showed the same effects as the global network. As for the DMN, there was also an STR_M and STR_SD increase from T3 to T4, but these values did not differentiate T1 and T4. This means that, during the EOEC transition, STR_M and STR_SD evolution lasts also after point 0 s; no such effect was seen during the ECEO transition.
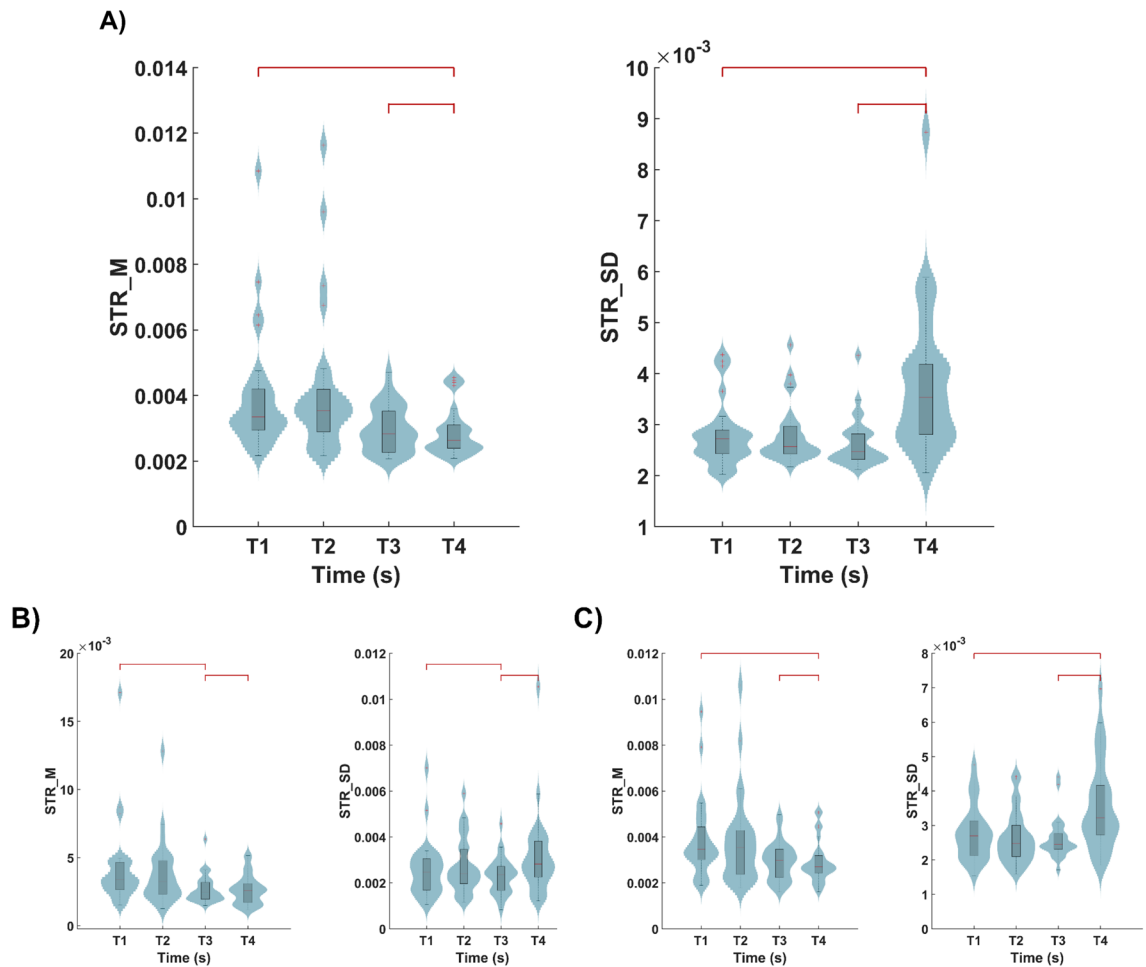
Figure 6. (**A**) Data distribution of the global network STR_M, and STR_SD during the EOEC transition in the alpha band. Analogous comparisons for the results regarding DMN and CEN are depicted in sections (**B,C**), respectively. Within each panel, the boxplots group the FC values of a different time range: from − 3 to − 1.5 s (T1), from − 1.5 to 0 s (T2), from 0 to 1.5 s (T3), and from 3 to 4.5 s (T4). The statistically significant differences (*p*-value < 0.05, corrected Wilcoxon signed-rank test) are indicated with dark red lines.

Again, no significant effects concerned EOEC transition in the beta band (see Supplementary material).

EO1Back transition

The Supplementary material contain the results of the EC1Back transition analysis. These analyses indicate a significant reduction in the FC strength and variability. This transition involves eye-opening, which, as shown by the results presented above, leads to an FC decrease. Therefore, here only EO1back transition has been presented in detail.

Figure 7 presents the neural network topology, followed by the STR_M and STR_SD dynamics, during the EO1Back transition. Opposed to the condition consisting of eyes opening and closing, in this case, no significant changes in both FC metrics can be discerned. Furthermore, the range of topological changes in the intervals before and after the change of the condition is very similar and expresses almost the same dynamics as the time-varying FC within one state. As depicted in Fig. 8, no significant statistical effects were obtained.

Supplementary Material includes these analyses for the beta frequency. As in the alpha band, no significant quantitative or qualitative effects were observed.

1BackEO transition

The Supplementary Material contain the results of the 1BackEC transition analysis. These analyses indicate a significant increase in the FC strength and variability. This transition involves eye-closing, which, as shown by the results presented above, leads to an FC augmentation. Therefore, here only 1backEO transition has been presented in detail.

Figure 9 depicts the network global organization related to 1BackEO transition. It shows high FC dynamics, however, these time-varying patterns seem not to be significantly affected by the transition between 1-Back and EO conditions. This concerned diffuse network topology but also mean STR_M and STR_SD. What is more, no effects occurred at the level of separated DMN or CEN networks.
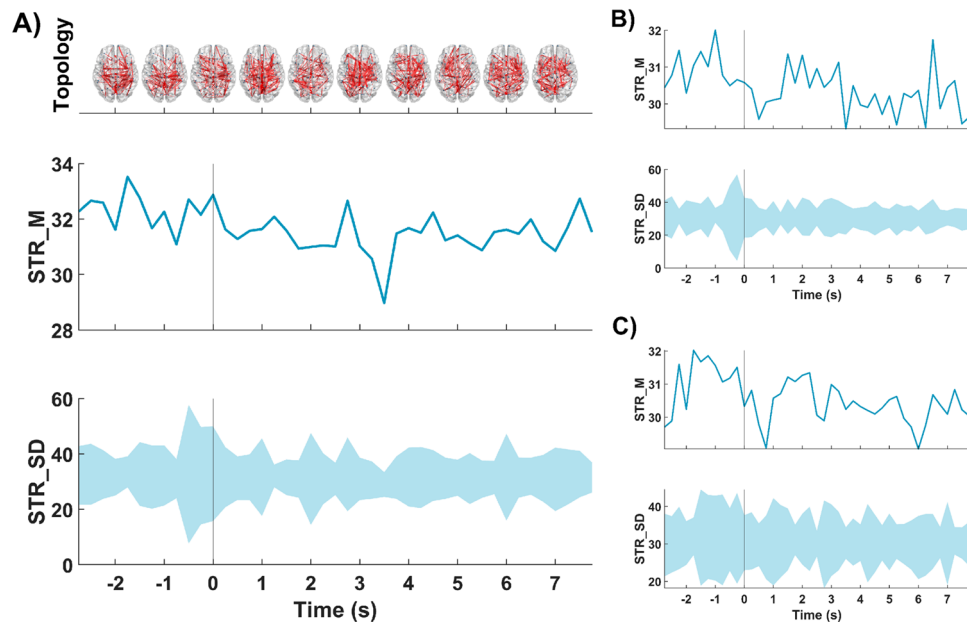
Figure 7. Evolution across time of the STR_M and STR_SD for: (**A**) global neural network, (**B**) DMN and (**C**) CEN. Within each section, in the upper row it is depicted the evolution of the STR_M, and in the lower row the evolution of the STR_SD during the EO1Back transition in the alpha band. The transition between both states is marked with a vertical line (i.e., 0 s). Moreover, for the global neural network, the evolution of the topology during the transition is depicted in the upper part of the section (**A**).

As could be predicted, the statistical analysis regarding mean STR_M and STR_SD values in the four analyzed intervals did not show any significant effects at the level of global networks, as well as for DMN or CEN (Fig. 10).

Discussion

The goal of our study was to model the expected time-organized reconfiguration of EEG-dependent functional connectivity, quantified in terms of the mean value and its variability, during the processes of transition between selected brain states. It was presumed that significant connectivity changes will appear during eyes closing and opening and during the transition between rest and a task-state[3,10]. Referring to these assumptions, we wanted to identify potential specificity and differences between selected types of transitions in terms of their duration and possible stages of change. The results showed that significant modifications in functional connectivity concerned transitions between eyes opening and closing and eyes-closed rest and a task state in the alpha frequency.

Although posterior alpha waves reactivity during eye opening and closing has been documented many decades earlier[50,51], our study reconstructed the sparsely explored temporally organized course of connectivity changes occurring during these transitions. As for eyes opening, the transition consisted of a fast decrease in coupling strength. PLI downturn occurred globally and at the level of selected network labeled as on-task and off-tasks. Besides overall synchronization strength, also its variability level decreased. This phenomenon means the process of connections alignment, which, taking into account the network topology changes, was possible due to the weakening of the highly centralized posterior hubs that dominated the eyes closed state. These changes took less than 1 s, suggesting that global connectivity functional pruning associated with eye-opening is a fast brain process. An important observation was that connectivity modification during eyes closing was not a mirror image of the ECEO reconfiguration. In the EOEC transition, connectivity strength and its variance increased. However, of special importance here is that this modulation was evidently slower than in the case of the ECEO networks shift, as indicated by the statistically significant differences in STR_M and STR_SD regarding the two intervals following the transition (i.e., time point = 0 s). The topology of the time-varying network also expressed different reorganization speed, as indicated by the formation of the posteriorly-centralized topology 3 s after eyes closing. Considering these findings, it seems likely that the global network's modulations ongoing during ECEO and EOEC exhibit different reorganization times. Connectivity changes recorded during eyes opening and closing considered the global network, as well as DMN and CEN suggesting the involvement of many neuronal structures not limited to the occipital cortex. Our outcomes are in line with other findings showing that, at the functional connectivity level, the differences between EO and EC states account for many other regions and specific networks[10,11]. Han and co-workers[52] reported that differences regarding EO and EC states considered salience network, dorsal attention network, and selected motor and perceptual networks. Particularly, a connectivity strength increase during the EC state was reported. However, there are also some opposite findings suggesting an increase of coupling in DMN during EO condition; although in this case, authors referred mainly to posterior structures overlapping with the occipital cortex[16]. The decrease in alpha band power observed in EEG recordings during eye opening has been usually interpreted as disinhibition of the occipital cortex, enabling
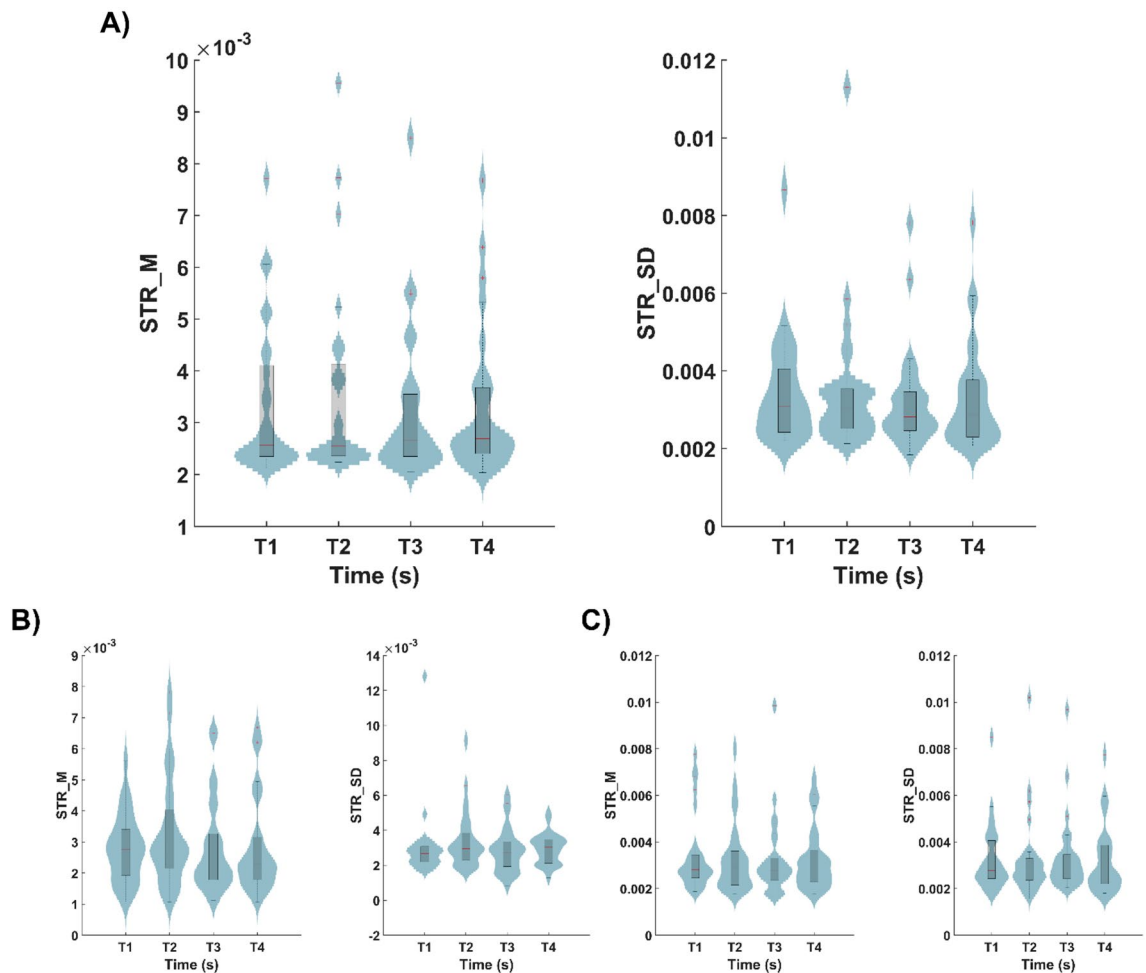
Figure 8. (**A**) Data distribution of the global network STR_M, and STR_SD during the EO1Back transition in the alpha band. Analogous comparisons for the results regarding DMN and CEN are depicted in sections (**B**,**C**), respectively. Within each panel, the boxplots group the FC values of a different time range: from −3 to −1.5 s (T1), from −1.5 to 0 s (T2), from 0 to 1.5 s (T3), and from 3 to 4.5 s (T4).

the processing of visual stimuli[53]. The results of network research suggest that the difference between EO and EC brain configurations reflect rather global dimensions associated with an exteroceptive state of attention and vigilance (EO) or interoception and mental imagery (EC)[10,54]. Also, Nakano et al.[55], in a series of original experiments with blinking, evidenced that even momentary eyes closing is associated with redirecting brain states into internally-oriented mental processing. In this context, our findings documenting a rapid global connectivity shift just after eye-opening might suggest a transition towards a state of readiness and alertness with potentially high evolutionary significance.

Subsequent analyses concerned neural network rearrangement between the rest and the task state. The transition from eyes-closed-rest to a task state contains eye-opening, a process of connectivity modulation described earlier; therefore, we focused on eyes-open-rest into task transition. As presented in the Supplementary Material, a network conversion from eyes-closed-to-task was associated with significant connectivity changes. The only negative finding concerned EO-task transition. This result can be explained by referring to several issues, including the methodological solutions used in our study. Firstly, the task (1-Back), although chosen deliberately, could be too easy, causing a lack of significant network reconfiguration. However, it seems unlikely due to the fact that even when performing a relatively simple task, the mere fact of the need to engage attentional mechanisms outwards should be sufficient to activate the task-on network[56]. Positive findings indicating significant differences between on-task and off-task networks come from studies in which many tasks of various complexity levels were used to elicit task-dependent brain activity[8]. This seems to be an ideal solution in such research because a given state-dependent network arrangement is not related to one task specificity. Unfortunately, such an approach could not be used in our study because it would require showing instructions each time and going through trial tasks, which would ultimately humper recording the transition from rest to task activity. Secondly, the majority of previous studies on differences between off-task and on-task neural networks were conducted using fMRI, a method measuring a different type of signal than EEG. Additionally, FC values based on fMRI and EEG are grounded on distinctive computational methods, which raises a question about the translatability of research outcomes regarding network transfigurations[57]. There is an ongoing debate about the compatibility of
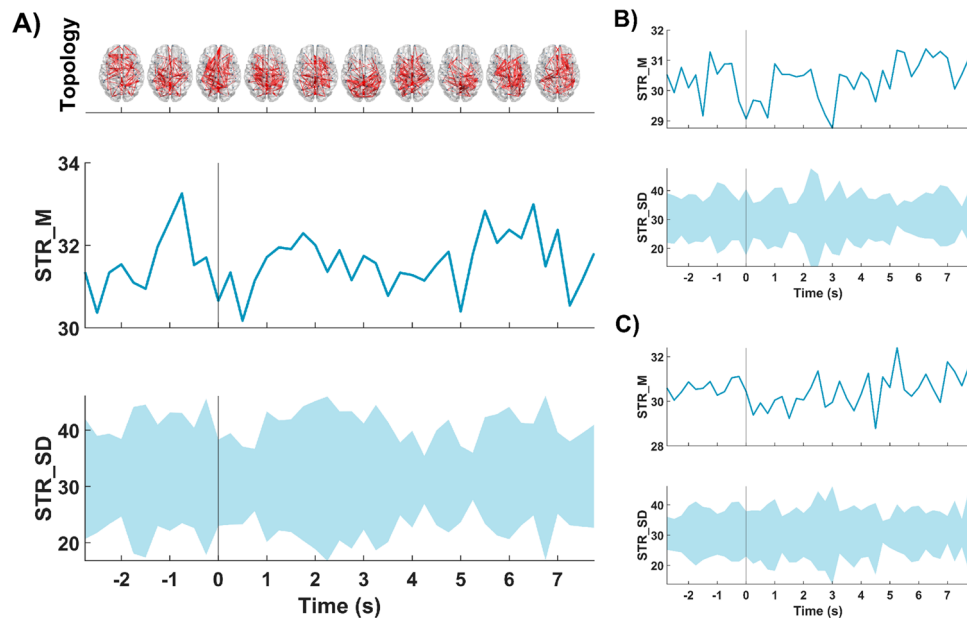
Figure 9. Evolution across time of the STR_M and STR_SD for: (**A**) global neural network, (**B**) DMN and (**C**) CEN. Within each section, in the upper row it is depicted the evolution of the STR_M, and in the lower row the evolution of the STR_SD during the 1BackEO transition in the alpha band. The transition between both states is marked with a vertical line (i.e., 0 s). Moreover, for the global neural network, the evolution of the topology during the transition is depicted in the upper part of the section (**A**).

time-organized connectivity patterns coming from fMRI and EEG, and the conclusions are not still unequivocal, considering that some studies indicate significant positive relationships[58], while others point out substantial differences[59,60]. Therefore, it cannot be ruled out that the lack of significant FC modification during EO-task transition is related to the EEG specificity and that studies using other neuroimaging modalities would obtain different results in this respect. Although the influence of mentioned methodological solutions on presented outcomes cannot be completely ruled out, what may be considered a limitation of the study, a more thorough literature review suggests other explanations. In previous studies comparing neural networks estimated in rest and task states, a certain tendency is noticeable, adding new insight into our results. In some of these researches, a 'rest' condition was recorded with eyes open[8,61–63], in others with eyes closed[6,64,65], and, in another, there was no information on this matter[2]. A typical trend in studies with eyes-open rest was to highlight similarities between rest and task networks, while substantial differences concerned mainly the studies with eyes closed resting-state, or when the rest condition was non-specified. Considering the above, it seems likely that if EO-rest and task-related networks have congruent features, no significant transition between them would occur, at least at the level of basic measures such as connectivity strength and variability.

Obtaining significant results regarding between-states network transition in the alpha band seems consistent with other research on the alpha oscillation functional characteristics. Brancaccio et al.[66] showed that transitions from wakefulness with eyes closed to light sleep were also associated with selective modulation of neuronal activity limited to the alpha band. This result suggests that the discussed frequency of neuronal oscillations may have a relatively universal function in the transitions between different states of the nervous system and is not only related to closing and opening the eyes. Other studies[67,68] confirmed the regulatory impact of prestimulus alpha oscillation on top–down control of attentional processes; for example, de Vries and co-workers[69] suggested that alpha band plays a significant role in regional tuning of the neuronal excitability facilitating selective attention even before the stimuli onset; Wöstmann and co-workers' study brought similar conclusions[70]. The association between alpha frequency and attentional readiness may also indirectly explain the lack of significant network modulations between the eyes-open (EO) resting state and the task state in our study. Taking into account the mentioned findings linking the alpha band with the readiness to filter and receive stimuli, it cannot be ruled out that in the EO state the level of brain preparation is already present; therefore, the transition to the task no longer requires a fundamental network reorganization in this frequency.

Before drawing conclusions some potential shortcomings of this study should be addressed. To our knowledge, the constructed experimental protocol was correct, but due to the fact that the applied processual analysis was carried out for the first time, it is possible that this protocol could be improved in future studies, e.g. regarding the number of between-state transition repetitions. However, it is possible that significantly increasing repetitions of task exposure could also lead to cognitive habituation, attenuating differences between rest and task-related networks. The lack of effects in frequencies other than alpha does not mean the complete absence of network transitions at frequencies such as delta and theta. Analyses comprising low frequencies may yield new results; however, we presumed that combining connectivity measures from a very wide frequency spectrum
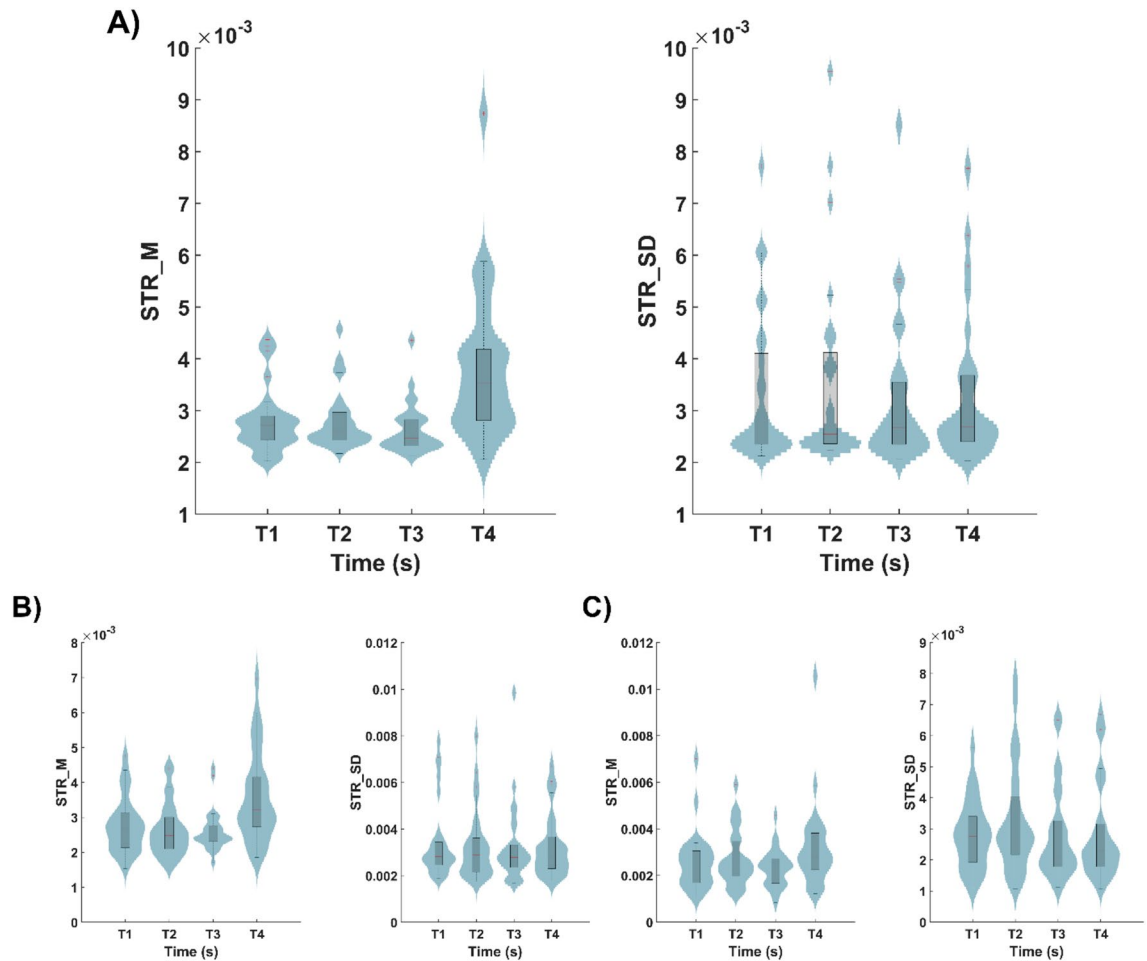
Figure 10. (**A**) Data distribution of the global network STR_M, and STR_SD during the 1BackEO transition in the alpha band. Analogous comparisons for the results regarding DMN and CEN are depicted in sections (**B**,**C**), respectively. Within each panel, the boxplots group the FC values of a different time range: from -3 to -1.5 s (T1), from -1.5 to 0 s (T2), from 0 to 1.5 s (T3), and from 3 to 4.5 s (T4).

may impede setting time intervals comparable for low and high frequency bands. Moreover, assessing the signal lateralization will also be interesting considering the involvement of the right hemisphere in the executive control and attentional functions[71] that may be important when starting a task. Finally, it seems reasonable to include a much larger study group in future research on the organization of neural network transitions, also to obtain greater statistical power.

Conclusions

This exploratory investigation showed that the multifaceted rearrangement of time-varying neural networks with eyes opening and closing exhibits a characteristic temporal dimension. Specifically, eyes opening was associated with a faster reconfiguration of brain activity globally, and also in selected functional networks. Although this is a matter of speculation, we believe that fast 'pruning' and alignment of functional connections when opening the eyes may have an evolutionary condition, in that the induction of a state of readiness to receive external information seems to be more conducive to the identification of environmental threats. Although our study brought some new findings and introduced a relatively original approach to analyzing network reconfiguration preserving linear temporal structure, a recapitulation and verification of results is necessary due to the specificity of the used methodology. Further studies should also establish the potential role of task difficulty while reconstructing network transition between rest and task states. Task complexity itself might be subjective and depend on the cognitive status of a specific group, e.g. for various clinical populations (e.g. patients with Alzheimer's disease) the EO-1back transition may prove to be a substantial challenge, paradoxically evoking prominent network reconfiguration unnoted in a healthy sample[72]. All these possibilities of experimental manipulations suggest that the concept of time-organized network transition requires further intensive empirical verifications.

Data availability

The data used during this study are available from the corresponding author upon reasonable request.

References

1. Hasson, U., Nusbaum, H. C. & Small, S. L. Task-dependent organization of brain regions active during rest. *Proc. Natl. Acad. Sci. USA* **106**(26), 10841–10846 (2009).
2. Di, X., Gohel, S., Kim, E. H. & Biswal, B. B. Task versus rest-different network configurations between the coactivation and the resting-state brain networks. *Front. Hum. Neurosci.* **7**, 493. https://doi.org/10.3389/fnhum.2013.00493 (2013).
3. Sadaghiani, S., Poline, J. B., Kleinschmidt, A. & D'Esposito, M. Ongoing dynamics in large-scale functional connectivity predict perception. *Proc. Natl. Acad. Sci. USA* **112**(27), 8463–8468 (2015).
4. Reed, M. B. *et al.* Serotonergic modulation of effective connectivity in an associative relearning network during task and rest. *NeuroImage* **249**, 118887. https://doi.org/10.1016/j.neuroimage.2022.118887 (2022).
5. Shine, J. M. & Poldrack, R. A. Principles of dynamic network reconfiguration across diverse brain states. *Neuroimage* **180**(Pt B), 396–405 (2018).
6. Lynch, L. K. *et al.* Task-evoked functional connectivity does not explain functional connectivity differences between rest and task conditions. *Hum. Brain Mapp.* **39**(12), 4939–4948 (2018).
7. Arbabshirani, M. R., Havlicek, M., Kiehl, K. A., Pearlson, G. D. & Calhoun, V. D. Functional network connectivity during rest and task conditions: A comparative study. *Hum. Brain Mapp.* **34**, 2959–2971 (2013).
8. Cole, M. W., Bassett, D. S., Power, J. D., Braver, T. S. & Petersen, S. E. Intrinsic and task-evoked network architectures of the human brain. *Neuron* **83**(1), 238–251 (2014).
9. Petrican, R. & Levine, B. T. Similarity in functional brain architecture between rest and specific task modes: A model of genetic and environmental contributions to episodic memory. *Neuroimage* **179**, 489–504 (2018).
10. Costumero, V., Bueichekú, E., Adrián-Ventura, J. & Ávila, C. Opening or closing eyes at rest modulates the functional connectivity of V1 with default and salience networks. *Sci. Rep.* **10**(1), 9137. https://doi.org/10.1038/s41598-020-66100-y (2020).
11. Weng, Y. *et al.* Open eyes and closed eyes elicit different temporal properties of brain functional networks. *NeuroImage* **222**, 117230. https://doi.org/10.1016/j.neuroimage.2020.117230 (2020).
12. Agcaoglu, O., Wilson, T. W., Wang, Y. P., Stephen, J. & Calhoun, V. D. Resting state connectivity differences in eyes open versus eyes closed conditions. *Hum. Brain Mapp.* **40**, 2488–2498 (2019).
13. Riedl, V. *et al.* Local activity determines functional connectivity in the resting human brain: A simultaneous FDG-PET/fMRI study. *J. Neurosci.* **34**(18), 6260–6266 (2014).
14. Liu, X. *et al.* Dynamic properties of human default mode network in eyes-closed and eyes-open. *Brain Topogr.* **33**, 720–732 (2020).
15. Wang, X. H., Li, L., Xu, T. & Ding, Z. Investigating the temporal patterns within and between intrinsic connectivity networks under eyes-open and eyes-closed resting states: A dynamical functional connectivity study based on phase synchronization. *PLoS One* **10**(10), e0140300. https://doi.org/10.1371/journal.pone.0140300 (2015).
16. Wang, Y. *et al.* Open eyes increase neural oscillation and enhance effective brain connectivity of the default mode network: Resting-State electroencephalogram research. *Front. Neurosci.* **16**, 861247. https://doi.org/10.3389/fnins.2022.861247 (2022).
17. Abrol, A. *et al.* Replicability of time-varying connectivity patterns in large resting state fMRI samples. *Neuroimage* **163**, 160–176 (2017).
18. Lurie, D. J. *et al.* Questions and controversies in the study of time-varying functional connectivity in resting fMRI. *Netw. Neurosci.* **4**(1), 30–69 (2020).
19. Kucyi, A. & Davis, K. D. Dynamic functional connectivity of the default mode network tracks daydreaming. *Neuroimage* **100**, 471–480 (2014).
20. Núñez, P. *et al.* Abnormal meta-state activation of dynamic brain networks across the Alzheimer spectrum. *Neuroimage* **232**, 117898. https://doi.org/10.1016/j.neuroimage.2021.117898 (2021).
21. Cattarinussi, G., Di Giorgio, A., Moretti, F., Bondi, E. & Sambataro, F. Dynamic functional connectivity in schizophrenia and bipolar disorder: A review of the evidence and associations with psychopathological features. *Prog. Neuropsychopharmacol. Biol. Psychiatry* **127**, 110827. https://doi.org/10.1016/j.pnpbp.2023.110827 (2023).
22. Hearne, L. J., Cocchi, L., Zalesky, A. & Mattingley, J. B. Reconfiguration of brain network architectures between resting-state and complexity-dependent cognitive reasoning. *J. Neurosci.* **37**(35), 8399–8411 (2017).
23. Cheng, H. J. *et al.* Task-related brain functional network reconfigurations relate to motor recovery in chronic subcortical stroke. *Sci. Rep.* **11**(1), 8442. https://doi.org/10.1038/s41598-021-87789-5 (2021).
24. O'Neill, G. C. *et al.* Measurement of dynamic task related functional networks using MEG. *Neuroimage* **146**, 667–678 (2017).
25. Iraji, A. *et al.* Tools of the trade: Estimating time-varying connectivity patterns from fMRI data. *Soc. Cogn. Affect. Neurosci.* **16**(8), 849–874 (2021).
26. Gratton, C. *et al.* Functional brain networks are dominated by stable group and individual factors, not cognitive or daily variation. *Neuron* **98**(2), 439-452.e5 (2018).
27. Dixon, M. L. *et al.* Interactions between the default network and dorsal attention network vary across default subsystems, time, and cognitive states. *Neuroimage* **147**, 632–649 (2017).
28. Klein, E. *et al.* Anticipation of difficult tasks: neural correlates of negative emotions and emotion regulation. *Behav. Brain Funct.* **15**, 4. https://doi.org/10.1186/s12993-019-0155-1 (2019).
29. Portnova, G. V. *et al.* Autonomic and behavioral indicators on increased cognitive loading in healthy volunteers. *Neurosci. Behav. Phys.* **53**, 92–102 (2023).
30. Raven, J. The Raven's progressive matrices: Change and stability over culture and time. *Cogn. Psychol.* **41**(1), 1–48 (2000).
31. Jaworowska, A. & Szustrowa T. *Test Matryc Ravena w wersji Standard TMS. Formy: Klasyczna, Równoległa, Plus.* (Pracownia Testów Psychologicznych PTP, 2000).
32. Rodríguez-González, V. *et al.* Consistency of local activation parameters at sensor- and source-level in neural signals. *J. Neural Eng.* **17**(5), 056020. https://doi.org/10.1088/1741-2552/abb582 (2020).
33. Lai, M., Demuru, M., Hillebrand, A. & Fraschini, M. A comparison between scalp- and source-reconstructed EEG networks. *Sci. Rep.* **8**(1), 12269. https://doi.org/10.1038/s41598-018-30869-w (2018).
34. Pascual-Marqui, R. D. Standardized low-resolution brain electromagnetic tomography (sLORETA): Technical details. *Methods Find Exp. Clin. Pharmacol.* **24**(Suppl D), 5–12 (2002).
35. Kaur, C., Singh, P., Bisht, A., Joshi, G. & Agrawal, S. Recent developments in spatio-temporal EEG source reconstruction techniques. *Wirel. Personal. Commun.* **122**(2), 1531–1558 (2022).
36. Moon, J. U. *et al.* Comparative analysis of background EEG activity in juvenile myoclonic epilepsy during valproic acid treatment: a standardized, low-resolution, brain electromagnetic tomography (sLORETA) study. *BMC Neuro* **22**(1), 48. https://doi.org/10.1186/s12883-022-02577-6 (2022).
37. Nardone, R. *et al.* Usefulness of EEG techniques in distinguishing frontotemporal dementia from Alzheimer's disease and other dementias. *Dis. Markers* **2018**, 6581490. https://doi.org/10.1155/2018/6581490 (2018).
38. Tadel, F., Baillet, S., Mosher, J. C., Pantazis, D. & Leahy, R. M. Brainstorm: A user-friendly application for MEG/EEG analysis. *Comput. Intell. Neurosci.* **2011**, 879716. https://doi.org/10.1155/2011/879716 (2011).

39. Fonov, V., Evans, A., McKinstry, R., Almli, C. & Collins, D. Unbiased nonlinear average age-appropriate brain templates from birth to adulthood. *Neuroimage* **47**, S102. https://doi.org/10.1016/j.neuroimage.2010.07.033 (2009).
40. Douw, L., Nieboer, D., Stam, C. J., Tewarie, P. & Hillebrand, A. Consistency of magnetoencephalographic functional connectivity and network reconstruction using a template versus native MRI for co-registration. *Hum. Brain Mapp.* **39**(1), 104–119 (2018).
41. Gramfort, A., Papadopoulo, T., Olivi, E. & Clerc, M. OpenMEEG: Opensource software for quasistatic bioelectromagnetics. *Biomed. Eng. Online* **9**(1), 45. https://doi.org/10.1186/1475-925X-9-45 (2010).
42. Vidaurre, D. *et al.* Spectrally resolved fast transient brain states in electrophysiological data. *NeuroImage* **126**, 81–95 (2016).
43. Desikan, R. S. An automated labeling system for subdividing the human cerebral cortex on MRI scans into gyral based regions of interest. *Neuroimage* **31**(3), 968–980 (2006).
44. Bastos, A. M. & Schoffelen, J. M. A tutorial review of functional connectivity analysis methods and their interpretational pitfalls. *Front. Syst. Neurosci.* **9**(175), 1–23 (2016).
45. Stam, C. J., Nolte, G. & Daffertshofer, A. Phase lag index: Assessment of functional connectivity from multi channel EEG and MEG with diminished bias from common sources. *Hum. Brain Mapp.* **28**(11), 1178–1193 (2007).
46. Ruiz-Gómez, S. J. *et al.* Computational modeling of the effects of EEG volume conduction on functional connectivity metrics. Application to Alzheimer's disease continuum. *J. Neural Eng.* **16**(6), 066019. https://doi.org/10.1088/1741-2552/ab4024 (2019).
47. Nobukawa, S., Kikuchi, M. & Takahashi, T. Changes in functional connectivity dynamics with aging: A dynamical phase synchronization approach. *Neuroimage* **188**, 357–368 (2019).
48. Strijbis, E. M. *et al.* State changes during resting-state (magneto) encephalographic studies: The effect of drowsiness on spectral, connectivity, and network analyses. *Front. Neurosci.* **16**, 782474. https://doi.org/10.3389/fnins.2022.782474 (2022).
49. Benjamini, Y. & Hochberg, Y. Controlling the false discovery rate: A practical and powerful approach to multiple testing. *J. R. Stat. Soc. Ser. B Stat. Methodol.* **57**(1), 289–300 (1995).
50. Berger, H. Über das elektrenkephalogramm des menschen. *Eur. Arch. Psychiatry Clin. Neurosci.* **98**(1), 231–254 (1933).
51. Jasper, H. H. Cortical excitatory state and variability in human brain rhythms. *Science* **83**(2150), 259–260 (1936).
52. Han, J. *et al.* Eyes-open and eyes-closed resting state network connectivity differences. *Brain Sci.* **13**(1), 122. https://doi.org/10.3390/brainsci13010122 (2023).
53. Wan, L. *et al.* From eyes-closed to eyes-open: Role of cholinergic projections in EC-to-EO alpha reactivity revealed by combining EEG and MRI. *Hum. Brain Mapp.* **40**(2), 566–577 (2019).
54. Marx, E. *et al.* Eyes open and eyes closed as rest conditions: Impact on brain activation patterns. *Neuroimage* **21**(4), 1818–1824 (2004).
55. Nakano, T., Kato, M., Morito, Y., Itoi, S. & Kitazawa, S. Blink-related momentary activation of the default mode network while viewing videos. *Proc. Natl. Acad. Sci. USA* **110**(2), 702–706 (2013).
56. Kirschner, A., Kam, J. W., Handy, T. C. & Ward, L. M. Differential synchronization in default and task-specific networks of the human brain. *Front. Hum. Neurosci.* **6**, 139. https://doi.org/10.3389/fnhum.2012.00139 (2012).
57. Nentwich, M. *et al.* Functional connectivity of EEG is subject-specific, associated with phenotype, and different from fMRI. *Neuroimage* **218**, 117001. https://doi.org/10.1016/j.neuroimage.2020.117001 (2020).
58. Abreu, R., Simões, M. & Castelo-Branco, M. Pushing the limits of EEG: Estimation of large-scale functional brain networks and their dynamics validated by simultaneous fMRI. *Front. Neurosci.* **14**, 323. https://doi.org/10.3389/fnins.2020.00323 (2020).
59. Ayres-Ribeiro, F. *et al. Brain's Dynamic Functional Organization with Simultaneous EEG-fMRI Networks*. International Workshop on Complex Networks (pp. 1–13). (Springer Nature Switzerland, Cham, 2023).
60. Rizkallah, J., Amoud, H., Fraschini, M., Wendling, F. & Hassan, M. Exploring the correlation between M/EEG source-space and fMRI networks at rest. *Brain Topogr.* **33**(2), 151–160 (2020).
61. Madhyastha, T. M., Askren, M. K., Boord, P. & Grabowski, T. J. Dynamic connectivity at rest predicts attention task performance. *Brain Connect.* **5**(1), 45–59 (2015).
62. Kieliba, P., Madugula, S., Filippini, N., Duff, E. P. & Makin, T. R. Large-scale intrinsic connectivity is consistent across varying task demands. *PLoS One* **14**(4), e0213861. https://doi.org/10.1371/journal.pone.0213861 (2019).
63. Kraus, B. T. *et al.* Network variants are similar between task and rest states. *Neuroimage* **229**, 117743. https://doi.org/10.1016/j.neuroimage.2021.117743 (2021).
64. Li, R. *et al.* Developmental maturation of the precuneus as a functional core of the default mode network. *J. Cogn. Neurosci.* **31**(10), 1506–1519 (2019).
65. Li, F. *et al.* Reconfiguration of brain network between resting state and P300 task. *IEEE Trans. Cogn. Dev. Syst.* **13**(2), 383–390 (2021).
66. Brancaccio, A., Tabarelli, D., Bigica, M. & Baldauf, D. Cortical source localization of sleep-stage specific oscillatory activity. *Sci. Rep.* **10**, 6976. https://doi.org/10.1038/s41598-020-63933-5 (2020).
67. Klimesch, W., Sauseng, P. & Hanslmayr, S. EEG alpha oscillations: The inhibition-timing hypothesis. *Brain Res. Rev.* **53**, 63–88. https://doi.org/10.1016/j.brainresrev.2006.06.003 (2007).
68. Bagherzadeh, Y., Baldauf, D., Pantazis, D. & Desimone, R. Alpha synchrony and the neurofeedback control of spatial attention. *Neuron* **105**(3), 577-587.e5. https://doi.org/10.1016/j.neuron.2019.11.001 (2020).
69. de Vries, I. E. J., Marinato, G. & Baldauf, D. Decoding object-based auditory attention from source-reconstructed MEG alpha oscillations. *J. Neurosci.* **41**(41), 8603–8617. https://doi.org/10.1523/JNEUROSCI.0583-21.2021 (2021).
70. Wöstmann, M., Maess, B. & Obleser, J. Orienting auditory attention in time: lateralized alpha power reflects spatio-temporal filtering. *Neuroimage* **228**, 117711 (2021).
71. Spagna, A., Kim, T. H., Wu, T. & Fan, J. Right hemisphere superiority for executive control of attention. *Cortex* **122**, 263–276. https://doi.org/10.1016/j.cortex.2018.12.012 (2020).
72. Schumacher, J. *et al.* Dynamic functional connectivity changes in dementia with Lewy bodies and Alzheimer's disease. *Neuroimage Clin.* **22**, 101812. https://doi.org/10.1016/j.nicl.2019.101812 (2019).

Author contributions

P.K., V.R-G., J.P., N.K-P., C.G. wrote the main manuscript V.R-G. prepared the figures P.K., N.K-P. performed the study V.R-G., J.P., C.G. conduct the data analyses.

Funding

Competing interests

The authors declare no competing interests.

Additional information

Supplementary Information The online version contains supplementary material available at https://doi.org/10.1038/s41598-024-68532-2.

Correspondence and requests for materials should be addressed to P.K.

Reprints and permissions information is available at www.nature.com/reprints.

Publisher's note Springer Nature remains neutral with regard to jurisdictional claims in published maps and institutional affiliations.